

SUPPLEMENTAL MATERIALS

Supplemental Methods

In vitro assessment of pioglitazone on MMP-9 protein expression in murine macrophages

Mouse peritoneal macrophages (MPMs) were isolated from C57BL/6J mice (Jackson Laboratories, Bar Harbor, ME). MPMs were isolated 4 days after intraperitoneal injection of 4% aged thioglycollate broth (Sigma, St. Louis, MO). MPMs were pelleted and resuspended in RPMI 1640 medium (Sigma). Cells of equal number (a total of 5×10^6 cells in each well) were seeded in 6-well plates and incubated at 37°C for 2 hours before gentle rinsing to remove nonadherent cells. Adherent MPMs were maintained in RPMI 1640 medium containing 10% heat-inactivated fetal bovine serum.

To examine the effect of pioglitazone on MMP-9 protein secretion from murine macrophages, MPMs were pretreated with pioglitazone hydrochloride (10 μ M, Takeda Pharmaceuticals North America, Lincolnshire, IL) for 18 hours, and then stimulated with lipopolysaccharide (LPS, 100 ng/mL, Sigma) for a period of 24 hours (PIO+,LPS+). Separate control groups using equal numbers of cells included 1) MPMs without any manipulation (PIO-, LPS-) and 2) MPMs stimulated with LPS for 24 hours (PIO-, LPS+). Cell culture supernatants from each of the three groups were collected and concentrated to the same volume using Amicon ultra-15 filters (Millipore, Billerica, MA). A total of 20 μ L of concentrated culture supernatants was loaded into each lane for

immunoblotting. Experiments were performed in triplicate. Band intensity was quantified by densitometry of immunoblots using ImageJ (version 1.36b, NIH Bethesda, MD). Equal supernatant protein loading from each group of was verified by Ponceau S staining of membranes.

Spectrally distinct MMP and macrophage imaging agents for in vivo fluorescence molecular imaging.

Carotid plaque MMP activity was imaged using a near-infrared fluorescence (NIRF) MMP-activatable probe (MMPSense680, 200 nmol/kg, ex/em 680nm/700nm, Visen Medical, Bedford, MA) with avidity for plaque gelatinases.¹ Macrophage phagocytic activity was detected utilizing a spectrally distinct macrophage-avid dextranated nanoparticle (CLIO-Cy7, 10 mg Fe/kg, ex/em 750 nm/800 nm, MGH-CMIR, Boston, MA).² At the time of imaging, a third spectrally resolved fluorescence agent, FITC-dextran (MW 2,000,000, 10 mg/kg, ex/em 494 nm/521 nm, Sigma), was injected to provide a vascular angiogram outlining carotid arterial plaques.

Intravital fluorescence microscopy

IVFM studies employed a multichannel laser scanning fluorescence microscope (IV 330, Olympus Corp, Tokyo, Japan) equipped with 3 laser lines (488-, 633-, and 748-nm excitation) and optimized for intravital imaging. The utilized 4x objective (NA 0.15) provided an in-plane resolution of 13×13 μm. Z-stacks (30-50 slices) were obtained at 10 μm steps through the vessel. A plastic tube phantom (PE-10 tubing, Becton Dickinson, Franklin Lakes, NJ) was placed underneath carotid artery bifurcation and

served to co-register the imaging fields of the 2 IVFM datasets. Excitation with three laser lines and image collection of the different channels were interleaved to minimize crosstalk between channels. All image settings were kept constant for all time points and samples.

Image analysis

Image analysis of IVFM data sets was performed by compiling z-stacks into a 2-dimensional summation image (ImageJ, version 1.36b, Bethesda, MD). Plaques were further colocalized as filling defects on FITC-dextran generated angiograms. Regions-of-interest (ROIs) were manually traced within the plaque and the adjacent normal vessel as previously.³⁻⁵

The total NIRF signal in the ROI was calculated as the summation of the signal intensity (SI) of all pixels in the ROI. The plaque target-to-background ratio (TBR) was calculated as the ratio of plaque SI to the adjacent vessel background SI. The plaque MMP and macrophage TBRs were measured in each respective channel. If a carotid plaque was not visualized on baseline IVFM, the animal was excluded from the study. The change in TBR (Δ TBR) for each respective NIRF channel was defined as the difference in TBR between 2nd IVFM and 1st IVFM.

Histopathology

After sacrifice, mice were perfused with 0.9% saline (20 mL) via the left ventricle. For histopathological analysis, excised right carotid arteries and aortic roots were

embedded in optimal cutting temperature compound (Sakura Finetek, Torrance, CA), and the remainder of the aorta was snap-frozen for Western blot analysis. Serial 6- μm -thick cryostat sections were obtained from embedded aortic roots and carotid arteries for fluorescence microscopy. Adjacent sections were stained with hematoxylin and eosin (H&E) for general morphology and Masson's trichrome for collagen.

Immunohistochemistry on adjacent sections was performed for macrophages (anti-mouse Mac3, BD Biosciences, San Jose, CA) and MMP-9 (anti-mouse MMP-9, Abcam Inc., Cambridge, MA), using avidin-biotin peroxidase method. Briefly, sections treated with 0.3% hydrogen peroxide were incubated for 60 minutes with a primary antibody, followed by respective biotinylated secondary antibody. The reaction was visualized with a 3-amino-9-ethyl-carbazol substrate (AEC, Sigma), and counterstained with Harris hematoxylin solution. Adjacent sections treated with nonimmune IgG provided controls for antibody specificity.

Quantitative histological measurements of plaque sections

Stained tissue sections were viewed with a microscope (Nikon Eclipse 50i, Tokyo, Japan), and images were digitally captured with a CCD-SPOT RT digital camera (Diagnostic Instruments, Sterling Heights, MI). Measurements were performed on IPLab imaging software (version 3.9.9; Scanalytics Inc., Rockville, MD). The %MMP-9 and %macrophage areas were defined as the respective positive immunostained areas divided by the total carotid plaque area (2 sections from each of the 13 animals, 26 total sections). Quantification of aortic lesion areas (mm^2) was performed using the software

program ImageJ (NIH). Calibration of digital aortic plaque images was performed using an image of a hemacytometer slide, where 1 mm was determined to equal to 1600 pixels. The aortic plaque area was calculated as the area between the internal elastic lamina and the lumen on H&E sections (3 sections from each of the 13 animals, 39 total sections). The percent collagen area on aortic plaque sections was defined as the percentage of positive staining area per total plaque area in Masson's trichrome stained sections.

Fluorescence microscopy

Fluorescence microscopy was performed on fresh-frozen carotid atheromata sections using an upright epifluorescence microscope (Nikon Eclipse 80i, Tokyo, Japan) interfaced with a cooled CCD camera (Cascade, Photometrics, AZ). Fluorescence images were obtained at a wavelength of far red (filter, 650 ± 22.5 nm excitation; 710 ± 25 nm emission, Q680LP bandpass, exposure time 1.0 second), or near-infrared (filter, 775 ± 25 nm excitation; 845 ± 27.5 nm emission, Q810LP bandpass, exposure time 30.0 seconds), to visualize the distribution of MMPsense680 (MMP activity) or CLIO-Cy7 (macrophage activity) fluorescence in plaque sections, respectively.

Immunoblot analysis

For mouse peritoneal macrophages, MMP-9 immunoblotting was performed using a goat monoclonal antibody (1:1000, R&D Systems, Minneapolis, MN) applied to concentrated supernatants.

For immunoblotting of aortic vessel lysates, frozen aortas were first pulverized, added to RIPA buffer (50 mM Tris, 150 mM NaCl, 1% Nonidet P-40, 0.5% sodium deoxycholate, 0.1% sodium dodecyl sulfate) with freshly added protease inhibitors, and centrifuged (10 minutes, 13,000 rpm, 4°C). Next the protein extract was boiled in electrophoresis buffer for 10 minutes, followed by the separation on 10% polyacrylamide gels under reducing conditions (β -mercaptoethanol) and transfer onto Immobilon-P membranes (Millipore) using semi-dry transfer (2 hr, 18V). After nonspecific binding sites were blocked for 1 hour with 5% delipidated milk in TBST (20 mM Tris, 55 mM NaCl, and 1% Tween 20), immunoblotting for MMP-9 (1:1000, R&D Systems) and macrophages (anti-mouse LAMP-2, 1:200, Santa Cruz Biotechnology, Santa Cruz, CA) was performed using chemiluminescence (PerkinElmer Life Sciences, Boston, MA).

Measurement of plasma metabolic and lipid parameters

At the time of sacrifice, blood was obtained for the measurement of plasma glucose, cholesterol and triglyceride levels using commercial colorimetric assay kits (Wako chemicals, Richmond, VA). Plasma insulin was measured with a murine ELISA kit (Crystal Chem, Downers Grove, IL) according to the manufacturer's protocol.

Statistical analyses

Statistical analyses were performed with GraphPad Prism (v5.0; GraphPad Software, San Diego, CA). Data are expressed as mean \pm SEM. Densitometry measurements of MMP-9 signal on MPM immunoblots were assessed by ANOVA testing and followed by a post-hoc Tukey's test for multiple comparisons. The unpaired Student's' t-test was

used to test differences in the Δ TBR between the two groups, and was used for histological and immunoblotting parameters. The paired Student's' t-test was used to assess differences in the plaque TBRs between IVFM#1 and IVFM#2 within each group (HCD and HCD+PIO). Pearson correlation coefficients (r-values) were calculated for correlations between the Δ MMP TBR and Δ Mac TBR for the entire group, the HCD+PIO group, and the HCD group. A p-value of less than 0.05 was considered statistically significant.

SUPPLEMENTAL REFERENCES

1. Deguchi JO, Aikawa M, Tung CH, Aikawa E, Kim DE, Ntziachristos V, Weissleder R, Libby P. Inflammation in atherosclerosis: Visualizing matrix metalloproteinase action in macrophages in vivo. *Circulation*. 2006;114:55-62.
2. Jaffer FA, Nahrendorf M, Sosnovik D, Kelly KA, Aikawa E, Weissleder R. Cellular imaging of inflammation in atherosclerosis using magnetofluorescent nanomaterials. *Mol Imaging*. 2006;5:85-92.
3. Aikawa E, Nahrendorf M, Figueiredo JL, Swirski FK, Shtatland T, Kohler RH, Jaffer FA, Aikawa M, Weissleder R. Osteogenesis associates with inflammation in early-stage atherosclerosis evaluated by molecular imaging in vivo. *Circulation*. 2007;116:2841-2850.
4. Jaffer FA, Kim DE, Quinti L, Tung CH, Aikawa E, Pande AN, Kohler RH, Shi GP, Libby P, Weissleder R. Optical visualization of cathepsin k activity in atherosclerosis with a novel, protease-activatable fluorescence sensor. *Circulation*. 2007;115:2292-2298.
5. Pande AN, Kohler RH, Aikawa E, Weissleder R, Jaffer FA. Detection of macrophage activity in atherosclerosis in vivo using multichannel, high-resolution laser scanning fluorescence microscopy. *J Biomed Opt*. 2006;11:021009.

SUPPLEMENTAL TABLE

	HCD	HCD+PIO	<i>P value</i>
Body Weight (g)	25.4±0.3	25.5±0.5	0.8
Glucose (mg/dL)	98.7±7.9	93.9±9.4	0.71
Insulin (pg/mL)	335.9±41.9	226.5±31.3	0.1
Total Cholesterol (mg/dL)	747.7±32.3	519.6±39.7	0.0009
Triglyceride (mg/dL)	86.3±6.0	92.8±8.8	0.56

TABLE. Metabolic parameters of control (HCD) and pioglitazone-treated (HCD+PIO) apoE^{-/-} mice. Values are expressed as mean±SEM. HCD= high cholesterol diet, PIO=pioglitazone.

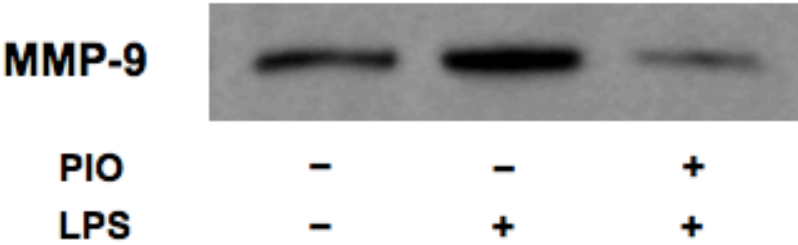
SUPPLEMENTAL FIGURE LEGENDS

Supplemental Figure S1. In vitro assessment of pioglitazone on matrix metalloproteinase (MMP)-9 protein expression in murine peritoneal macrophages (MPMs). (A) Immunoblot analysis of MMP-9 protein expression in supernatants of MPMs pre-treated with or without pioglitazone (10 μ M, 18hr) before lipopolysaccharide (LPS; 100 ng/mL, 24hr) stimulation. The immunoblot is representative of three independent experiments. (B) Densitometry analyses revealed that LPS-mediated MMP-9 expression was attenuated by pioglitazone pretreatment ($P<0.05$).

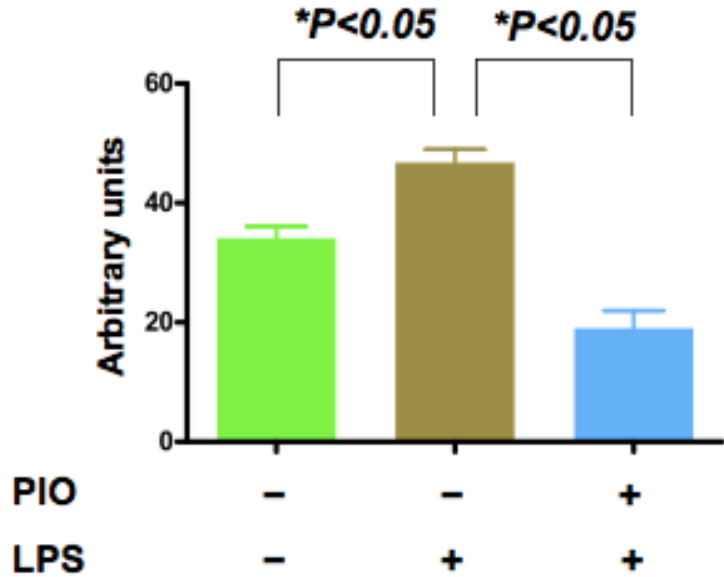
Supplemental Figure S2. Pioglitazone reduced plaque collagen content (as assessed by Masson's trichrome stain) in both (A) carotid and (B) aortic atheromata. HE, H&E-hematoxylin and eosin stain; MT=Masson's trichrome stain for collagen.

SUPPLEMENTAL FIGURE S1

A.



B.



SUPPLEMENTAL FIGURE S2

